# Section 1

# WIMP as a dark matter

In this section, we review the properties of WIMPs as DM. It is revealed, when we take a close look at the relic abundance of WIMP DM in Sec. 1.1, that a WIMP with the TeV scale mass is a good DM candidate, which is sometimes called *WIMP miracle* and is a strong motivation to consider WIMPs. In Sec. 1.2 and 1.3, we will consider two different ways to search for the WIMP DM, called the indirect and direct detection. Finally, Sec. 1.4 is devoted to the summary and concluding remarks of this section.

## 1.1 WIMP DM relic abundance

One of the most important evidences of the beyond SM is the existence of DM [1]. DM is an unknown object that occupies a non-negligible ratio of the total energy of our universe, but has not yet been directly observed because of its weak interaction with the SM particles.[♮1] In spite of its invisibility, the existence of DM is confirmed by several astrophysical observations such as the mass measurement using the gravitational lensing effect caused by galaxies and clusters [2, 3], the flatness of galactic rotation curves further the optical radius [4, 5], the measurement of the power spectrum of the cosmic microwave background (CMB), and so on. In particular, the observation of CMB allows us the precise determination of various cosmological parameters [6,7] including the density of the non-relativistic matter and baryon, which is currently determined as [8]

$$\Omega_m h^2 = 0.1430 \pm 0.0011, \tag{1.1}$$

$$\Omega_b h^2 = 0.02237 \pm 0.00015, \tag{1.2}$$

where $h \sim \mathcal{O}(1)$ is the Hubble constant in units of $100\,\mathrm{km\,s^{-1}\,Mpc^{-1}}$. The difference between $\Omega_m h^2$ and $\Omega_b h^2$ implies the existence of DM and its abundance $\Omega_\chi h^2 \simeq 0.12$.

In cosmology, DM production mechanisms that try to explain the DM abundance are divided into two main categories: thermal and non-thermal production. The former assumes the equilibrium between the DM and the thermal bath in the early universe. As the universe expands, the interaction rate that maintains the thermal equilibrium becomes smaller and the DM decouples from the thermal bath at some time, which is the so-called *freezeout*. As we will see below, the resulting abundance of the DM in this scenario is mainly controlled by the temperature of the thermal bath $T_f$ when the freezeout occurs. On the other hand,

[♮1] At worst DM interacts with the SM particles through the gravity, which is considerably weaker than all the other known interactions. **(♣ Mention to Ema paper?? ♣)**

non-thermal production assumes the DM production by some processes irrespective of the thermal bath such as decay of a heavy particle. Since the thermal production scenario can be realized in relatively simple setup and WIMPs are well motivated in connection with this kind of scenario, we focus on it.

We assume the stable DM particle $\chi$ with mass $m_\chi$ can pair annihilate into SM particles with some cross section $\sigma$. When DM is in thermal equilibrium with the thermal bath of temperature $T$, DM velocity obeys the collesponding Boltzmann distribution. Let $v$ be the relative velocity of annihilating DM particles and $\langle \sigma v \rangle$ be the thermal average of the product of $\sigma$ and $v$. By using this quantity, we can write down the Boltzmann equation for the DM number density $n_\chi$ as

$$\frac{d(n_\chi a^3)}{dt} = -a^3 \langle \sigma v \rangle (n_\chi^2 - n_{\rm eq}^2), \tag{1.3}$$

where $t$ and $a$ are the time coordinate and the scale factor, respectively, of the Friedmann Robertson Walker metric

$$ds^2 = -dt^2 + a(t)^2 d\boldsymbol{x}^2, \tag{1.4}$$

while $n_{\rm eq}$ denotes the number density of DM in equilibrium. When DMs are non-relativistic, its temperature dependence is given by $n_{\rm eq} \propto T^{3/2} \exp(-m_\chi/T)$. The first term of the right handed-side of Eq. (1.3) represents the annihilation rate of DM pairs that should be proportional to $n_\chi^2$, while the second term describes the DM creation through the inverse process. As desired, the number density does not change in time if $n_\chi = n_{\rm eq}$. Recalling the total entropy conservation in a comoving volume $sa^3 = (\text{const})$, it turns out to be convenient to define the ratio $Y \equiv n_\chi/s$. In fact, this modification cancels the effect of the expansion of the universe $\dot{a} > 0$ from Eq. (1.3), leading to a simpler equation

$$\frac{dY}{dt} = -s \langle \sigma v \rangle (Y^2 - Y_{\rm eq}^2), \tag{1.5}$$

with $Y_{\rm eq} \equiv n_{\rm eq}/s$.

Here we assume that the freezeout occurs when the relativistic radiation dominates the total energy of the universe, which will be verified to be correct later. In this case, we can derive $a \propto T^{-1}$ from the entropy conservation with $s \propto T^3$. For the numerical calculation, we define a dimensionless parameter $x \equiv m_\chi/T$. Then we can rewrite Eq. (1.5) as

$$\frac{x}{Y_{\rm eq}} \frac{dY}{dx} = -\frac{\Gamma}{H} \left( \frac{Y^2}{Y_{\rm eq}^2} - 1 \right), \tag{1.6}$$

where $\Gamma$ denotes the DM interaction rate defined as

$$\Gamma \equiv n_{\rm eq} \langle \sigma v \rangle . \tag{1.7}$$

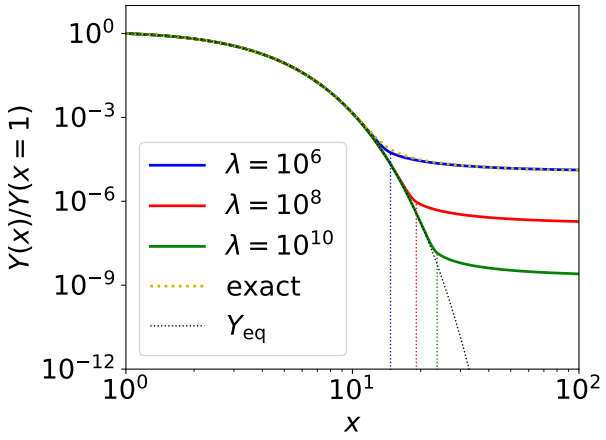


Figure 1: Plot of $Y(x)/Y(x=1)$ with $Y(x)$ being a solution of the evolution equation Eq. (1.6). The yellow dotted line is a solution for $\lambda \equiv \Gamma/H|_{x=1} = 10^6$, while the black dotted line denotes $Y_{\rm eq}(x)/Y_{\rm eq}(x=1)$. The solid lines are the approximation to the solutions described in the text. The blue, red, and green colors correspond to $\lambda = 10^8$, $10^{10}$, and $10^{12}$, respectively. The vertical dotted lines denote the freezeout temperature $x_f$.

Finally, $\langle\sigma v\rangle$ is known to be expanded as [9]

$$\langle\sigma v\rangle = \langle\sigma v\rangle_s + \langle\sigma v\rangle_p x^{-1} + \cdots , \tag{1.8}$$

collesponding to the $s$-wave, $p$-wave, and so on, contributions to the cross section. When $x \gg 1$, the term with the highest power of $x$ dominates the cross section. When the $x^{-p}$ term dominates ($p \geq 0$), temperature dependence of the interaction rate is $\Gamma \propto x^{-3/2-p}e^{-x}$, while the Hubble parameter only reduces as $H \propto \rho^{1/2} \propto x^{-2}$. As a result, at some point $\Gamma$ becomes smaller than $H$ and $Y$ freezes out as Eq. (1.6) indicates. Hereafter, we focus on the case of the $s$-wave domination with $\langle\sigma v\rangle_s \neq 0$ for simplicity. **(♣ What is the difference for $p$-wave and so on? ♣)** In Fig. 1, we show the solution of Eq. (1.6) for $\lambda \equiv \Gamma/H|_{x=1} = 10^6$ by the yellow dotted line. In the calculation, we use the boundary condition $Y(x=1) = Y_{\rm eq}(x=1)$ and plot the normalized value $Y(x)/Y(x=1)$. We also plot the function $Y_{\rm eq}(x)/Y_{\rm eq}(x=1)$ by the black dotted line.

Unfortunately, it is computationally hard to solve Eq. (1.6) for larger values of $\lambda$ because of the almost complete cancellation between two terms of the right handed side for small $x \sim \mathcal{O}(1)$ and its amplification caused by large $\lambda$. We adopt instead to use an approximation that is the same with the one adopted in the public code `MicrOMEGAs` [10, 11]. For the small $x$ region, temperature is still high enough to maintain the equilibrium $Y \simeq Y_{\rm eq}$, which means that $d\Delta Y/dx \ll dY_{\rm eq}/dx$ with $\Delta Y \equiv Y - Y_{\rm eq}$. From this approximation we obtain a formula

$$\Delta Y \simeq -\frac{x}{2\lambda}\frac{dY_{\rm eq}}{dx}. \tag{1.9}$$

Then we define the time $x_f$, or equivalently the so-called freezeout temperature $T_f$, when the approximation becomes invalid through the equation

$$\Delta Y(x_f) = 2.5 Y_{\rm eq}(x_f). \tag{1.10}$$

After the freezeout $x > x_f$, the annihilation of the DM pairs rapidly slows down and the DM abundance far exceeds its equilibrium value: $Y \gg Y_{\rm eq}$. Then we can neglect the second term of the right hand of Eq. (1.6) and obtain the analytical solution

$$Y(x) \simeq -\frac{x}{c_1 x + \lambda / Y_{\rm eq}(x=1)}, \tag{1.11}$$

where $c_1$ is a integration constant. In Fig. 1, we show results obtained with these two approximations Eqs. (1.9) and (1.11) for $\lambda = 10^6$ (blue), $10^8$ (red), and $10^{10}$ (green). In particular, the blue and the yellow lines almost completely overlaps with each other, which proves the validity of the approximations. The vertical dotted lines in the figure show the freezeout temperature. It can be seen from the figure that $x = x_f$ does correspond to the time when $Y$ starts to deviate from $Y_{\rm eq}$. Note also that as $\lambda \propto \langle \sigma v \rangle$ becomes larger, the freezeout time becomes later and the late time relic abundance becomes smaller.

When the DM properties (*i.e.*, the mass $m_\chi$ and the annihilation cross section $\langle \sigma v \rangle$) are given, corresponding relic abundance can be calculated using above procedure. In particular, $m_\chi$ determines the normalization of the figure, namely $Y_{\rm eq}(x=1) = Y_{\rm eq}(T = m_\chi)$, and $\langle \sigma v \rangle$ determines the freezeout temperature through the combination of Eq. (1.7). Assuming the absence of non-thermal effect, only some good combination of these two values should explain the current relic abundance of the DM. From the numerical calculation, we obtain an order estimation formula

$$\Omega_\chi h^2 \sim \frac{3 \times 10^{-27}\,{\rm cm}^3/{\rm s}}{\langle \sigma v \rangle_0} \sim 0.1 \left(\frac{0.01}{\alpha}\right)^2 \left(\frac{m_\chi}{300\,{\rm GeV}}\right)^2, \tag{1.12}$$

where the rough estimation $\langle \sigma v \rangle \sim \alpha^2 / m_\chi^2$ is used in the last equation with $\alpha$ being the fine structure constant for the DM-SM coupling. What is fascinating in Eq. (1.12) is that an object can be a DM candidate if it has mass comparable to the electroweak scale and coupling constant comparable to the electroweak coupling constant. This is the so-called *WIMP miracle*, which suppport the hypothesis of the WIMP as a cadidate of the DM. Such TeV-scale WIMPs are theoretically well-motivated in connection with problems of the SM such as the naturalness problem as reviewed in Sec. **??**.

**(♣ Virial velocity, mass density of DM, velocity of sun etc ♣)**

## 1.2 WIMP DM search : indirect detection

**(♣ Briefly review later ♣)**

## 1.3 WIMP DM search : direct detection

There are also many experiments aimed for the direct detection of the DM.[♮2] Here, we again assume some interaction between the DM and SM particles and look for a recoil of a target SM particle due to the collision with the DM in the laboratory. In the case of WIMPs of our concern, any particle with non-zero electroweak charge can be a target particle, which interacts with WIMPs through the $t$-channel electroweak gauge boson exchange. In the traditional setup such as the XENON1T experiment [13], a nucleus (of xenon in this case) and an electron are the frequently used target particles. **(♣ Cite electron scattering ♣)**.

## 1.4 Summary

**(♣ To search for WIMPs that do not compose a sizable fraction of the DM, we have to rely on the collider search. ♣)**

# References

[1] F. Zwicky, Die Rotverschiebung von extragalaktischen Nebeln, Helvetica Physica Acta 6 (1933) 110.

[2] F. Zwicky, On the Masses of Nebulae and of Clusters of Nebulae, Astrophysical Journal 86 (1937) 217.

[3] V. Trimble, Existence and Nature of Dark Matter in the Universe, Ann. Rev. Astron. Astrophys. 25 (1987) 425–472. doi:10.1146/annurev.aa.25.090187.002233.

[4] H. W. Babcock, The rotation of the Andromeda Nebula, Lick Observatory Bulletin 19 (1939) 41–51. doi:10.5479/ADS/bib/1939LicOB.19.41B.

[5] K. G. Begeman, A. H. Broeils, R. H. Sanders, Extended rotation curves of spiral galaxies: Dark haloes and modified dynamics, Mon. Not. Roy. Astron. Soc. 249 (1991) 523.

[6] G. Jungman, M. Kamionkowski, A. Kosowsky, D. N. Spergel, Weighing the universe with the cosmic microwave background, Phys. Rev. Lett. 76 (1996) 1007–1010. arXiv:astro-ph/9507080, doi:10.1103/PhysRevLett.76.1007.

[7] G. Jungman, M. Kamionkowski, A. Kosowsky, D. N. Spergel, Cosmological parameter determination with microwave background maps, Phys. Rev. D54 (1996) 1332–1344. arXiv:astro-ph/9512139, doi:10.1103/PhysRevD.54.1332.

[♮2] For the recent review of the direct detection experiments, see for example [12].

[8] N. Aghanim, et al., Planck 2018 results. VI. Cosmological parameters (2018). arXiv:1807.06209.

[9] P. Gondolo, G. Gelmini, Cosmic abundances of stable particles: Improved analysis, Nucl. Phys. B360 (1991) 145–179. doi:10.1016/0550-3213(91)90438-4.

[10] G. Bélanger, F. Boudjema, A. Pukhov, A. Semenov, MicrOMEGAs: A Program for calculating the relic density in the MSSM, Comput. Phys. Commun. 149 (2002) 103–120. arXiv:hep-ph/0112278, doi:10.1016/S0010-4655(02)00596-9.

[11] G. Bélanger, F. Boudjema, A. Goudelis, A. Pukhov, B. Zaldivar, micrOMEGAs5.0 : Freeze-in, Comput. Phys. Commun. 231 (2018) 173–186. arXiv:1801.03509, doi:10.1016/j.cpc.2018.04.027.

[12] T. Marrodán Undagoitia, L. Rauch, Dark matter direct-detection experiments, J. Phys. G43 (1) (2016) 013001. arXiv:1509.08767, doi:10.1088/0954-3899/43/1/013001.

[13] E. Aprile, et al., Dark Matter Search Results from a One Tonne×Year Exposure of XENON1T, Phys. Rev. Lett. 121 (11) (2018) 111302. arXiv:1805.12562, doi:10.1103/PhysRevLett.121.111302.